INVESTIGATION OF THE COMPOSITION AND STRUCTURE OF WAELZ SLAG

Angel Iliev[1], Nikolai Gogov[1], Daniela Grigorova[1], Gyunver Hodjaoglu[2]

[1]University of Chemical Technology and Metallurgy, 8 Kl. Ohridsky blvd., 1756 Sofia, Bulgaria; E-mail: d.dimitrova@uctm.edu
[2]Institute of Physical Chemistry "Acad. R. Kaischew", Bulgarian Academy of Sciences, Acad. G. Bonchev Str., block 11, 1113 Sofia; E-mail: gyunver@ipc.bas.bg
Corresponding author: d.dimitrova@uctm.edu

ABSTRACT. Waelz slag is a by-product generated during the high-temperature treatment of various zinc containing metallurgical residues in rotary kilns, most commonly through the Waelz process. This study focuses on the comprehensive characterisation of three types of Waelz slag (WS), each generated as a by-product of zinc extraction from a distinct processing route employing different charge materials: electric arc furnace dust (EAFD), zinc cakes from hydrometallurgical leaching, and lead smelting slags treated pyrometallurgically. The aim was to assess their potential for sustainable utilisation. The analyses included chemical composition, particle size distribution, phase identification through X-ray diffraction (XRD), and morphological assessment via scanning electron microscopy (SEM). Magnetic separation and density measurements were also performed to evaluate the material's processability. The results revealed significant variations in elemental composition, grain size distribution, porosity, and magnetic behaviour among the samples. High iron and calcium contents suggest potential applications in metallurgy and cement production, while elevated porosity and silicate content support possible use in construction materials. These investigations provide a foundation for the development of targeted recycling strategies in line with circular economy principles, reducing the need for landfill disposal and enabling the valorisation of industrial by-products.

Key words: Waelz slag; clinker, electric arc furnace dust; iron, structure.

Introduction

The Waelz process is a widely used high-temperature pyrometallurgical method for recovering zinc from various zinc-bearing industrial residues. In this process, the charge - typically a mixture of waste material and a reducing agent such as coke is introduced into a rotary kiln operating at temperatures between 1000 °C and 1200 °C. Zinc oxides are reduced to metallic zinc, which evaporates and is later oxidised and collected as zinc-rich dust (Kozlov, 2002; Xue et al., 2022). The primary outputs of the Waelz process are Waelz oxide (a secondary raw material for zinc production) and Waelz slag (WS), also referred to as Waelz clinker. While the terms "slag" and "clinker" are often used interchangeably, "clinker" may emphasize the sintered, granular physical structure of the residue, similar to cement clinker (Barella et al., 2014; Grudinsky et al., 2023). The Best Available Techniques (BAT) Reference Document for the Non-Ferrous Metals Industries classifies this residue as slag (European Commission, 2017).

WS is not generated exclusively from EAFD processing. It is also produced from other industrial zinc-bearing residues, such as zinc-leaching cakes and lead smelting slags, depending on the type of charge material introduced into the kiln. For example, WS may result from the treatment of classical hydrometallurgical zinc cakes, as well as from the Waelz processing of residues derived from pyrometallurgical lead metallurgy. Globally, approximately 600–800 kg of Waelz slag is produced per tonne of processed EAFD, which contributes to an estimated 1.75 million tonnes of WS generated annually (Salas et al., 2021; Grudinsky et al., 2023). The majority of this slag is still disposed of in landfills, posing long-term environmental risks and increasing economic costs. This reality is increasingly incompatible with current sustainability goals and the transition to a circular economy model.

Several studies have explored the potential reuse of WS in various applications, including civil engineering, road construction, and ceramic materials (Vegas et al., 2008; Quijorna et al., 2011, 2012; Abbà et al., 2017; Cifrian et al., 2019). However, high levels of heavy metals often limit its use due to environmental regulations on leaching behaviour (Barna et al., 2000). Other research has focused on WS use as a cement additive, a mineralizer, or a source of iron in clinker production (Durastanti and Moretti, 2024; Kuandykova et al., 2024), or explored methods of recovering valuable metals from WS through reductive smelting (Grudinsky et al., 2023). Despite these efforts, a universally applicable and sustainable utilisation strategy for WS has yet to be established. Most approaches remain limited in scale or scope, and comprehensive understanding of the material's phase and chemical composition is often lacking.

This study aims to provide a detailed characterisation of three different types of Waelz slag derived from distinct technological processes and charge materials. The findings are intended to support the development of more sustainable, application-specific recycling strategies for this industrial residue.

Materials and Methods

In this study, three types of Waelz slag were investigated, each obtained from a separate technological line within the Waelz process at a metallurgical plant in Bulgaria. The slag samples differ in both the type of charge material used and the specific technological parameters under which the Waelz process was conducted. The samples are described according to the main type of charge material used in each Waelz process:

- 1KCT – generated from pelletized electric arc furnace dust;

• 2KFCO – produced from the treatment of zinc cakes obtained through sulphuric acid leaching of zinc concentrates in a classical hydrometallurgical extraction scheme;
• 3KPB – derived from lead-bearing slags resulting from pyrometallurgical lead production.

The chemical composition of the samples was determined by atomic absorption analysis (AAA) and inductively coupled plasma spectroscopy (ICP) after digestion. The particle size distribution was determined by standard dry sieve analysis using a mechanical shaker and a graded set of sieves, following international testing procedures (ISO, 2012). True (pycnometric) density was measured to assess material compactness and porosity, while bulk density was evaluated to provide information relevant for material handling and process design (ISO, 2008; ISO, 2010).

Phase composition and mineralogical structure were identified via X-ray diffraction (XRD) using a PANalytical Empyrean diffractometer. In addition, three-dimensional internal structure was assessed through computed X-ray microtomography, providing information on pore connectivity and internal heterogeneity. Microstructural and surface features were examined by scanning electron microscopy (SEM) on a Zeiss EVO 10 system, operated with SmartSem Version 7.05 (Service Pack 3). Magnetic separation was carried out using a laboratory dry drum separator under a field intensity of approximately 0.3 Tesla. The mass fractions of magnetic and non-magnetic components were recorded to estimate the content of magnetically responsive phases, mainly iron oxides, and to evaluate their potential for metallurgical recovery.

Results and Discussion

The chemical composition of the three investigated Waelz slag samples is presented in Table 1. The results show significant differences in elemental content among the three samples, reflecting the specific charge materials and process parameters used in each process line. All three samples exhibit elevated contents of SiO_2, Al_2O_3, CaO, and MgO, which are typical for Waelz slags and are consistent with the formation of silicate-rich mineral phases. The moisture content across the samples ranged between 9% and 12%, which is typical for materials stored under ambient conditions.

Table 1. *Concentrations of characteristic components in the Waelz slag samples*

Parameter	Unit	1KCT	2KFCO	3KPB
Zn	%	0.24	0.63	0.45
Fe	%	31.86	5.57	4.2
Cu	%	0.47	0.72	0.42
Pb	%	0.06	0.37	0.35
As	%	-	0.16	0.11
Sb	%	0.042	0.05	0.16
SiO_2	%	10.81	23.01	34.85
Al_2O_3	%	4.2	5.89	7.63
CaO	%	28.63	25.3	28.35
MgO	%	3.06	26.70	2.29
Cl	%	0.007	0.04	0.002
F	%	0.18	0.028	0.028
Ge	g/t	11	10	10
Se	g/t	10	5	18
Te	g/t	5	8	5

XRD analyses of the samples are shown in Figures 1 to 3.

Sample 1KCT is characterised by high iron content (31.86% Fe) and elevated CaO (28.63%), with SiO_2 content (10.81%). These values align well with the XRD analysis (Figure 1), which identifies dominant crystalline phases as dicalcium silicate (Ca_2SiO_4), wüstite (FeO), portlandite ($Ca(OH)_2$), and metallic α-Fe. The presence of metallic iron suggests the slag formed under reducing conditions.

Sample 2KFCO exhibits a mineralogical profile dominated by serendibite ($CaMg_3Si_3O_{10}$, ~50%), along with gehlenite ($Ca_2Al_2SiO_7$), magnesite ($MgCO_3$), and minor iron oxide and metallic Fe (Figure 2). This is reflected in the chemical composition, with high contents of MgO (26.70%), CaO (25.3%), SiO_2 (23.01%), and moderate Al_2O_3 (5.89%). A minor Co-Mn sulphide phase (~14.7%) was also identified, confirming the presence of cobalt and manganese in trace amounts. These features are typical for slags formed from hydrometallurgically leached zinc cakes with complex mineralogical residues.

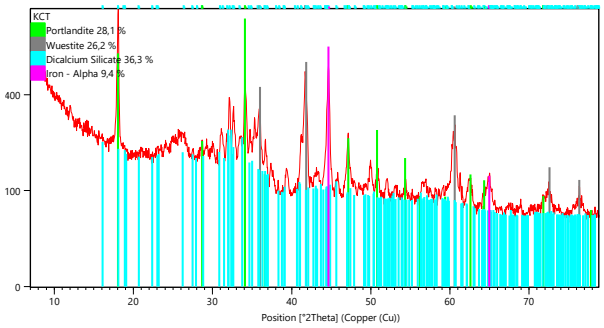


Fig. 1. XRD pattern of the 1KCT Waelz slag sample

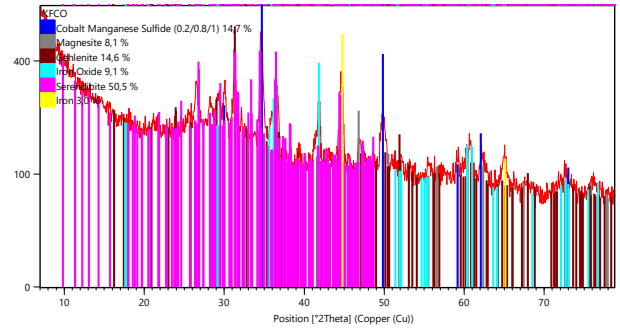


Fig. 2. XRD pattern of the 2KFCO slag sample

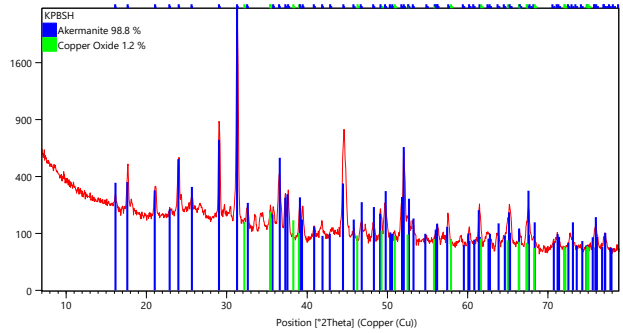


Fig. 3. XRD pattern of the 3KPB slag sample

Sample 3KPB shows the highest CaO (28.35%) and SiO_2 (34.85%) contents, with lower Fe (4.2%) and MgO (2.29%). While typical Waelz slag of this type may contain higher iron levels, in this particular case the iron content is reduced. The low iron content is explained by the use of lead paste as a

secondary charge material, which dilutes the iron input typical of this slag type. These values match the XRD pattern (Figure 3), which indicates the near-exclusive presence of akermanite ($Ca_2MgSi_2O_7$, ~98.8%), a stable calcium magnesium silicate phase. While Pb is present in the chemical analysis (0.35%), it is not represented in the crystalline phase composition most likely due to its occurrence in amorphous or low-crystallinity form. The results of the sieve analysis are presented in Figure 4 as discrete particle size fractions and in Figure 5 as cumulative retention curves for particles smaller than 1.4 mm.

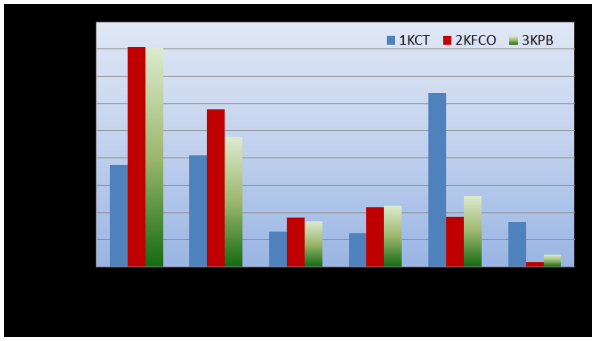


Fig. 4. Graph of particle distribution of samples of Waelz slag (clinker), %

All three Waelz slag samples exhibit a predominantly coarse-grained character, consistent with their clinker-like morphology. The majority of each sample's mass is concentrated in the coarsest fractions (>1.4 mm), with 51.91% for 1KCT, 83.88% for 2KFCO, and 89.44% for 3KPB. These results were confirmed by the cumulative distribution plots (Figure 5), showing the steep rise in retained mass above 1.4 mm. Sample 1KCT contains a more balanced distribution across the middle-size range, with 31.99% in the 1.4–0.63 mm fraction, and 18.75% in particles larger than 15 mm (Figure 4). In contrast, 2KFCO and 3KPB contain a significant portion of their mass in the coarse fractions: particles account for 40.36% and 28.98%, respectively. All three samples show minimal content of fine particles below 0.63 mm.

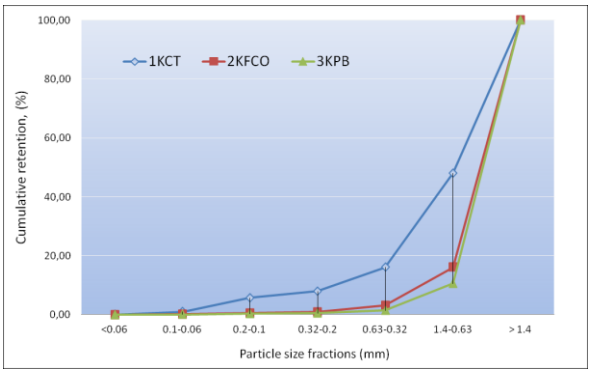


Fig. 5. Cumulative retention curves for samples

The magnetic separation results revealed substantial differences among the samples. The magnetic fraction accounted for 53.9% in sample 1KCT, 70.1% in 2KFCO, and 63.2% in 3KPB. Despite its lower iron content, 2KFCO exhibited the highest magnetic yield, which can be attributed to the coarse particle size and presence of magnesium silicates adhering to iron-rich grains. The magnetic fraction in 1KCT is consistent with its high Fe content and the presence of both metallic iron and wüstite, as identified in XRD analysis. For 3KPB, the magnetic portion is more influenced by grain size effects and minor iron-bearing inclusions than by overall Fe concentration.

The results obtained in the determination of bulk and pycnometric density, as well as porosity, are systematised and presented in Figure 6. The studied samples exhibit relatively low bulk density values, which is typical for porous, slag-like materials. The pycnometric density averages around 2.7 g/cm³, close to the theoretical values for silicates and iron or aluminium oxides. The observed differences between bulk and true densities are primarily attributed to internal porosity and the presence of entrapped voids within the slag particles.

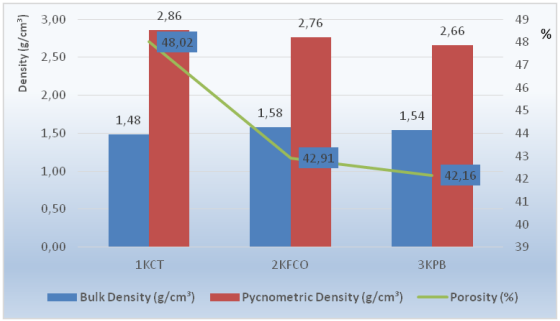


Fig. 6. Bulk density, pycnometric density, and calculated porosity of the Waelz slag samples

Among the samples, 2KFCO demonstrates the highest bulk density (1.58 g/cm³), suggesting a more compact bulk structure, most likely due to its coarse particle size distribution and relatively lower internal porosity (42.91%). In contrast, 1KCT shows the lowest bulk density (1.48 g/cm³) but the highest pycnometric density (2.86 g/cm³), indicating that while the material is intrinsically dense, it contains a significant amount of voids reflected in its highest porosity value (48.02%). Sample 3KPB occupies an intermediate position in terms of both density and porosity, with values consistent with its phase composition dominated by akermanite.

Figure 7 presents the SEM micrograph of the 1KCT Waelz slag sample, selected for detailed observation due to its high iron content (31.86%) and dominant iron-bearing phases (Fe, FeO) identified via XRD. The image shows irregular particles with uneven surfaces, typical of high-temperature residues. The morphology is characterised by angular grains and porous textures, confirming the previously measured high porosity (48.02%).

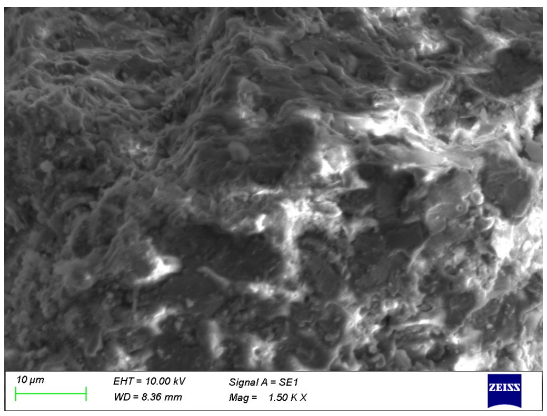


Fig. 7. SEM photomicrographs of 1KCT Waelz slag

Numerous micropores and intergranular voids are visible across the slag matrix, formed during gas evolution and

solidification under reducing conditions. These features, while typical for Waelz slag, are particularly prominent in 1KCT due to the combination of high Fe content and mineral phases such as wüstite and metallic iron. The presence of dense zones and fragmented inclusions with high contrast in the SEM image further supports the existence of metallic iron and iron-rich oxides, suggesting the material retains pyrometallurgical value. The physical structure - porous, yet containing recoverable dense phases, makes 1KCT a strong candidate for subsequent iron recovery or reductive melting processes.

The detailed physicochemical and mineralogical characterisation of the three Waelz slag samples highlights their distinct potential for targeted secondary applications, depending on their composition and structure:

- 1KCT, with its high iron content, presence of metallic iron and wüstite, and moderate porosity, is most suitable for pyrometallurgical reuse in the steelmaking and iron alloy industries. Its dense, iron-rich matrix makes it a promising raw material for iron recovery or as a reducing agent in metallurgical operations.
- 2KFCO, characterised by elevated levels of SiO_2, MgO, and Al_2O_3, along with complex silicate phases such as serendibite and gehlenite, is appropriate for ceramic and glass applications, particularly in the refractory and glass-ceramic sectors where chemical durability and high-temperature resistance are essential.
- 3KPB, dominated by akermanite, with a balanced content of CaO and SiO_2 and relatively low concentrations of leachable heavy metals, has high potential for use in construction materials - such as cement additives, paving stones, or eco-concretes - where its mineralogy and particle size support binding and durability.

Conclusion

This study provides a comprehensive characterisation of three types of Waelz slag, generated from distinct technological lines within a metallurgical plant. The samples differ significantly in chemical composition, phase assemblage, particle size distribution, density, and porosity features that are closely tied to the nature of the feed material and operational conditions of the Waelz process. Sample 1KCT demonstrated the highest iron content and a dense microstructure, making it particularly suitable for pyrometallurgical recovery of iron or use in iron-based alloys. Sample 2KFCO, rich in complex magnesium-aluminium silicates, shows potential for ceramic and refractory applications. Sample 3KPB, dominated by akermanite, aligns well with the requirements for cement and concrete production. Across all samples, porosity and oxide content support possible incorporation into construction or composite materials. The findings confirm that Waelz slag is not a homogeneous waste, but a material stream with varied and valuable characteristics. With proper classification and targeted processing, it can be redirected from landfilling towards resource-efficient industrial reuse. This aligns with circular economy strategies and supports sustainable materials management in the non-ferrous metallurgical sector.

Our results also provide a valuable foundation for further investigations into the thermodynamic behaviour of Waelz slag during non-isothermal heating under reducing conditions, aimed at optimising future reprocessing strategies.

References

Abbà, A., Sorlini, S. & Collivignarelli, M.C. (2017). Research experiences on the reuse of industrial waste for concrete production. *MATEC Web of Conferences*, *121,* Article 10001. https://doi.org/10.1051/matecconf/201712110001.

Barna, R., Bae, H.R., Méhu, J., Van der Sloot, H., Moszkowicz, P. & Desnoyers, C. (2000). Assessment of chemical sensitivity of Waelz slag. *Waste Management*, *20*(2–3), 115–124. https://doi.org/10.1016/S0956-053X(99)00310-4

Barella, M., Pagnanelli, F. & Toro, L. (2014). Laboratory investigation of Waelz slag stabilization. *Process Safety and Environmental Protection*, *92*(6), 659–667. https://doi.org/10.1016/j.psep.2014.06.015

Cifrian, E., Coronado, M. & Quijorna, N. (2019). Waelz slag-based construction ceramics: Effect of the trial scale on technological and environmental properties. *Journal of Material Cycles and Waste Management*, *21*, 1437–1448. https://doi.org/10.1007/s10163-019-00896-4

Durastanti, C. & Moretti, L. (2024). Assessing the climate effects of clinker production: A statistical analysis to reduce its environmental impacts. *Cleaner Environmental Systems*, *13,* Article 100204. https://doi.org/10.1016/j.cesys.2024.100204

European Commission (2017). *Best Available Techniques (BAT) Reference Document for the Non-Ferrous Metals Industries: Industrial Emissions Directive 2010/75/EU (Integrated Pollution Prevention and Control)*. Luxembourg: Publications Office of the European Union, p.163.

Grudinsky, P., Zinoveev, D., Kondratiev, A., Delitsyn, L., Kulumbegov, R., Lysenkov, A., Kozlov, P. & Dyubanov, V. (2023). Reduction smelting of the Waelz slag from electric arc furnace dust processing: An experimental study. *Crystals*, *13*(2), Article 318. https://doi.org/10.3390/cryst13020318

ISO, 2008–2012. Standards for metallic powder characterisation: ISO 3923-1:2008, ISO 3923-2:2010, ISO 13796:2012. Geneva: International Organisation for Standardisation.

Kozlov, P.A. (2002). *The Waelz Process*. Moscow: Ruda i Metally Publishing House. (In Russian)

Kuandykova, A., Taimasov, B., Potapova, E., Sarsenbaev, B., Kolesnikov, A., Begentayev, M., Kuldeyev, E., Dauletiyarov, M., Zhanikulov, N., Amiraliyev, B. & Abdullin, A. (2024). Production of composite cement clinker based on industrial waste. *Journal of Composites Science*, *8*(7), Article 257. https://doi.org/10.3390/jcs8070257

Quijorna, N., Coz, A., Andres, A. & Cheeseman, C. (2012). Recycling of Waelz slag and waste foundry sand in red clay bricks. *Resources, Conservation and Recycling*, *65,* 1–10. https://doi.org/10.1016/j.resconrec.2012.05.004

Salas, I., Cifrian, E., Andres, A. & Viguri, J.R. (2021). Self-organizing maps to assess the recycling of waste in ceramic construction materials. *Applied Sciences*, *11*(21), Article 10010. https://doi.org/10.3390/app112110010

Vegas, I., Ibañez, J.A., San José, J.T. & Urzelai, A. (2008). Construction demolition wastes, Waelz slag and MSWI bottom ash: A comparative technical analysis as material for road construction. *Waste Management*, *28*, 565–574. https://doi.org/10.1016/j.wasman.2007.01.016

Xue, Y., Hao, X., Liu, X. & Zhang, N. (2022). Recovery of zinc and iron from steel mill dust—An overview of available technologies. *Materials*, *15*(12), Article 4127 https://doi.org/10.3390/ma15124127